

Slow dynamics in gelation phenomena: From chemical gels to colloidal glasses

Emanuela Del Gado,^{a,d}, Annalisa Fierro,^{b,d}, Lucilla de Arcangelis,^{c,d} and Antonio Coniglio ^{b,d}

^a*Laboratoire des Verres, Université Montpellier II, 34095 Montpellier, France*

^b*Dipartimento di Scienze Fisiche, Università di Napoli "Federico II", Complesso Universitario di Monte Sant'Angelo, via Cintia 80126 Napoli, Italy*

^c*Dipartimento di Ingegneria dell'Informazione, Seconda Università di Napoli, via Roma 29, 81031 Aversa (Caserta), Italy and*

^d*INFM Udr di Napoli and Gruppo coordinato SUN*

(Dated: May 22, 2019)

We here discuss the results of 3d MonteCarlo simulations of a minimal lattice model for gelling systems. We focus on the dynamics, investigated by means of the time autocorrelation function of the density fluctuations and the particle mean square displacement. We start from the case of chemical gelation, i.e. with permanent bonds, we characterize the critical dynamics as determined by the formation of the percolating cluster, as actually observed in polymer gels. By opportunely introducing a finite bond life time τ_b the dynamics displays relevant changes and eventually the onset of a glassy regime. This has been interpreted in terms of a crossover to dynamics more typical of colloidal systems and a novel connection between classical gelation and recent results on colloidal systems is suggested. By systematically comparing the results in the case of permanent bonds to finite bond lifetime, the crossover and the glassy regime can be understood in terms of effective clusters.

I. INTRODUCTION

The gelation transition transforms a viscous liquid into an elastic disordered solid. In general this is due to the formation in the liquid phase of a spanning structure, which makes the system able to bear stresses.

In polymer systems, this is due to chemical bonding, that can be induced in different ways [1, 2], producing a polymerizations process. As firstly recognized by Flory, the change in the viscoelastic properties is directly related to the constitution inside the sol of a macroscopic polymeric structure, that characterizes the gel phase. In the experiments [3] the viscosity coefficient grows with a power law behavior, as function of the relative difference from the critical polymer concentration, characterized by a critical exponent k . The onset of the elastic response in the system, as function of the same control parameter, displays a power law increasing of the elastic modulus described by a critical exponent f . As implicitly suggested in the work of Flory and Stockmayer [1], the percolation model is considered as the basic model for the chemical gelation transition and the macromolecular stress-bearing structure in these systems is a percolating network [2, 4, 5]. The gelling solution in the experiments typically displays slow dynamics: the relaxation functions present a long time stretched exponential decay $\sim e^{-(\frac{t}{\tau_0})^\beta}$ as the gelation threshold is approached. In particular at the gel point the relaxation process becomes critically slow, and the onset of a power law decay is typically observed [6].

In many other physical systems where aggregation processes and structure formation take place, gelation phenomena can be observed. Typically, these are colloidal systems, i.e. suspensions of mesoscopic particles interacting via short range attraction. These systems are intensively investigated due to their relevance in many research fields (from proteins studies to food industry).

Due to the possibility in the experiments of opportunely tuning the features of the interactions, they also play the role of model systems.

Here strong attraction gives rise to a diffusion limited cluster-cluster aggregation process and may produce gel formation (colloidal gelation) at very low density as a spanning structure is formed [7]. The latter is generally quite different from the polymer gels case [8] but, for what the viscoelastic behavior is concerned, this gelation transition closely resembles the chemical one, observed in polymer systems [9]. With a weaker attraction at higher density a gelation characterized by a glass-like kinetic arrest [10, 11] may be observed. The relaxation patterns closely recall the ones observed in glassy systems and are well fitted by the mode-coupling theory predictions for super-cooled liquids approaching the glass transition [12]. On the theoretical side the application of the mode-coupling theory to systems with short range attractive interactions [13, 14, 15] (*attractive glasses*) has been recently considered and the connection with the colloidal glass transition has been proposed. The short range attraction enhances the caging mechanism characteristic of glassy regimes in hard sphere systems and produces a glassy behavior at lower densities, depending on the attraction strength.

At lower densities, the role of the structure formation, that is directly observed in some systems [16], might have a relevance in the dynamics but it has not been clarified yet. Also the eventual crossover to the glassy regime [9], as the density is increased, is not completely understood. In this paper we investigate the connection among colloidal gelation, colloidal glass transition and chemical gelation. Some preliminary studies have been reported in [17].

We have considered a minimal model for gelling systems and performed extensive numerical simulations on 3d cubic lattices. In Sect. II we give the details of the

model and of the simulations. In Sect.s III and IV the results relative to relaxation and diffusion properties are presented and discussed. In the last section some concluding remarks are given.

II. DESCRIPTION OF THE MODEL

A. Permanent bonds

Our model consists in a solution of monomers diffusing on a cubic lattice. As in most experimental systems in the case of polymer gels, we choose the monomers to be tetrafunctional. Each monomer occupies a lattice elementary cell, and therefore eight vertices on the lattice. To take into account the excluded volume interaction, two monomers cannot occupy nearest neighbors and next nearest neighbors cells on the lattice, i.e. nearest neighbor monomers cannot have common sites. At $t = 0$ we fix the fraction ϕ of present monomers respect to the maximum number allowed on the lattice, and randomly quench bonds between them. This actually corresponds to the typical chemical gelation process that can be obtained by irradiating the monomeric solution. We form at most four bonds per monomer, randomly selected along lattice directions and between monomers that are nearest neighbors and next nearest neighbors (namely bond lengths $l = 2, 3$). Once formed, the bonds are permanent.

For each value of ϕ there is an average value $N_b(\phi)$ of the fraction of formed bonds respect to all the possible ones, obtained by averaging over different initial configurations.

Varying ϕ the system presents a percolation transition at $\phi_c = 0.718 \pm 0.005$ [18]. The critical exponents for the percolation transition agree with the random percolation predictions [19] (e.g. for the mean cluster size $\gamma \simeq 1.8 \pm 0.05$ and for the correlation length $\nu \simeq 0.89 \pm 0.01$ in 3d [18]).

The monomers diffuse on the lattice via random local movements and the bond length may vary but not be larger than l_0 according to bond-fluctuation dynamics (BFD) [20], where the value of l_0 is determined by the self-avoiding walk condition. On the cubic lattice it is $l_0 = \sqrt{10}$ in lattice spacing units and the allowed bond lengths are $l = 2, \sqrt{5}, \sqrt{6}, 3, \sqrt{10}$ [21]. We let the monomers diffuse to reach the stationary state and then study the system for different values of the monomer concentration.

This lattice model with permanent bonds has been introduced to study the critical behavior of the viscoelastic properties at the gelation transition[22]. The relaxation time is found to diverge at the percolation threshold ϕ_c with a power law behavior [18]. The elastic response in the gel phase has been studied by means of the fluctuations in the free energy and goes to zero at ϕ_c with a power law behavior as well [23].

B. Bonds with finite lifetime

Colloidal gelation is due to a short range attraction and in general the particles are not permanently bonded. To take into account this crucial feature we introduce a novel ingredient in the previous model by considering a finite bond lifetime τ_b and study the effect on the dynamics.

The features of this model with finite τ_b can be realized in a microscopic model: a solution of monomers interacting via an attraction of strength $-E$ and excluded volume repulsion. Due to monomer diffusion the aggregation process eventually takes place. The finite bond lifetime τ_b corresponds to an attractive interaction of strength $-E$, where $\tau_b \sim e^{E/KT}$.

We start with the same configurations of the previous case, with a fixed ϕ where the bonds have been randomly quenched as described above. During the monomer diffusion with *BFD* at each time step we attempt to break each bond with a frequency $1/\tau_b$. Between monomers separated by a distance less than l_0 bonds are then formed with a frequency f_b [24]. In order to obtain monomers configurations that are similar to the ones with permanent bonds, for each value of τ_b we fix f_b so that the fraction of present bonds coincides with its average value in the case of permanent bonds, $N_b(\phi)$ [26].

With respect to the case of permanent bonds we notice that, as the finite bond lifetime τ_b corresponds to an attractive interaction of range l_0 , it actually introduces a correlation in the bond formation and may eventually lead to a phase separation between a low density and a high density phase: There is no evidence of phase separation for the values of τ_b and f_b considered in this paper. This is evident in Fig.1, where typical equilibrium configurations with $\phi = 0.6$ are shown in two different cases: in Fig.1(a) we have the case considered in this paper, obtained with $\tau_b = 100$ and $f_b = 0.02$; in Fig.1(b) with $\tau_b = 2$ and $f_b = 1$ the phase separation may occur. The choice of monomers of functionality 4, also in this case of finite bond lifetime, may correspond to a directional effect in the interaction [27].

The case of extremely large τ_b gives rise to different situations depending on the initial condition and the bond creation process. We consider two extreme cases: I) Start with the initial configuration where the monomers are randomly distributed, and the bonds are randomly quenched. At later times the frequency of forming bonds is zero. This case corresponds to the permanent bond case (chemical gelation), described in section II A. II) Start with a random configuration of monomers and let the monomers diffuse and form bonds with infinite lifetime and frequency f_b . This phenomenon of irreversible aggregation, with the occurrence of gelation after a spanning cluster is formed, corresponds to cluster-cluster aggregation class of models for $f_b = 1$ [28], with a tendency towards cluster-cluster reaction limited aggregation process [29] for $f_b < 1$. This out of equilibrium phenomenon can be representative of colloidal gelation and will not be considered here. In chemical gelation and colloidal

gelation the formation of the critical cluster should produce the slow dynamics. The main difference is due to the fact that the critical density and the temperature is much lower in colloidal gelation than in chemical gelation, and the fractal dimension is related to cluster-cluster aggregation models and not to random percolation.

Finally, in the limit of $\tau_b \rightarrow 0$, where one recovers free monomers, the model reproduces a lattice gas model and does not present any glassy behavior. In fact we do not recover in this limit (which corresponds to $T \rightarrow \infty$) the glass transition usually found in hard sphere models. Due to this feature we can be sure that the slow dynamics that we find in the model is only due to the presence of finite lifetime bonds.

III. RELAXATION FUNCTIONS

In order to investigate the dynamic behavior we study, for both the permanent bond and the finite bond lifetime case, the equilibrium density fluctuation autocorrelation functions $f_{\vec{q}}(t)$ given by

$$f_{\vec{q}}(t) = \frac{\langle \rho_{\vec{q}}(t + t') \rho_{-\vec{q}}(t') \rangle}{\langle |\rho_{\vec{q}}(t')| \rangle^2} \quad (1)$$

where $\rho_{\vec{q}}(t) = \sum_{i=1}^N e^{-i\vec{q} \cdot \vec{r}_i(t)}$, $\vec{r}_i(t)$ is the position of the i -th monomer at time t , N is the number of monomers and the average $\langle \dots \rangle$ is performed over the time t' . Due to the periodic boundary conditions the values of the wave vector \vec{q} on the cubic lattice are $\vec{q} = \frac{2\pi}{L}(n_x, n_y, n_z)$ with $n_x, n_y, n_z = 1 \dots L/2$ integer values. These functions have been calculated on a cubic lattice of size $L = 16$. The data have been averaged over ~ 10 up to 10^5 time intervals and over $\sim 20 - 30$ different initial configurations of the sample [30]. In the following we discuss the data obtained for $q \sim 1.36$ ($\vec{q} = (\pi/4, \pi/4, \pi/4)$). Qualitatively, analogous behaviors have been observed for different values of q . Undoubtedly, due to the structure formation over different length scale, a detailed study of the geometric properties and of the dynamics for different wave vectors might be relevant [31].

In the case of permanent bonds the system is considered at equilibrium when both the diffusion coefficient has reached its asymptotic limit, and the autocorrelation functions have gone to zero. For $\Phi < \Phi_c$ we are always able to thermalize the system, instead for $\Phi > \Phi_c$ it remains out of equilibrium, and it is possible that it is in an aging regime [31]. In Fig.2, $f_{\vec{q}}(t)$ is plotted as function of the time, for different values of the monomer concentration, with $q \sim 1.36$ and the data have been averaged over 40 different initial configurations of the sample. The different curves correspond to different values of ϕ , ranging from 0.5 to 0.85. At low concentrations the system completely relaxes within the simulation time, the relaxation process becomes slow as the concentration is increased and above the percolation threshold ϕ_c the system is kinetically arrested, in the sense that the relax-

ation functions do not go to zero within the time scale of the simulations.

We analyze more quantitatively the long time decay of $f_{\vec{q}}(t)$ in Fig.3: As the monomer concentration ϕ approaches the percolation threshold ϕ_c , $f_{\vec{q}}(t)$ displays a long time decay well fitted by a stretched exponential law $\sim e^{-(t/\tau)^\beta}$ with a $\beta \sim 0.30 \pm 0.05$. Intuitively, this behavior can be related to the cluster size distribution close to the gelation threshold, which produces relaxation processes taking place over different length scales. At the percolation threshold the onset of a power law decay is observed as it is shown by the double logarithmic plot of Fig.3 with an exponent c [6]. formation of the critical cluster, that actually determines the kinetic arrest. As the monomer concentration is increased above the percolation threshold in the gel phase, the long time power law decay of the relaxation functions can be fitted with a decreasing exponent c , varying from $c \sim 1$. at ϕ_c to $c \sim 0.2$ well above ϕ_c , where a nearly logarithmic decay appears. Again this suggests that the growth of the relaxation time is driven by the formation of the critical cluster, that actually determines the kinetic arrest. On the whole, this behavior well agrees with the one observed in gelling systems investigated in the experiments of refs.[6]. It is interesting to notice that this kind of decay with a stretched exponential and a power law reminds the relaxation behavior found in spin-glasses [32]. Many analogies in the dynamics of gels and spin-glasses have been recently pointed out [33], but the underlying physics is rather unclear.

In the model with finite lifetime bonds, the equilibration time is an increasing function of τ_b . The system is considered at equilibrium when both the average number of bonds has reached its asymptotic limit and the autocorrelation functions have gone to zero [34]. In this case very different behaviors are observed. In Fig.4 $f_{\vec{q}}(t)$ is plotted as function of time for a fixed value of $\tau_b = 10, 100, 1000$ (respectively Fig.4a, 4b and 4c) for increasing values of the monomer concentration (ϕ varies from below to well above $\phi_c = 0.718$). At low concentrations, the behavior of the autocorrelation function $f_{\vec{q}}(t)$ is apparently very similar to the one observed in the case of permanent bonds: the system completely relaxes within the simulations time scale and the relaxation time increases with the concentration ϕ . At high concentrations, a two-step decay appears, that closely resembles the one observed in super-cooled liquids. This qualitative behavior is observed for many different values of the bond lifetime τ_b . As the Fig. 4 show, the two step decay is more pronounced for higher values of τ_b .

In Fig.5 we focus on the long time decay of $f_{\vec{q}}(t)$ as the value ϕ_c of the monomer concentration is approached from below, for $\tau_b = 100$: the data are well fitted by a stretched exponential decay, with an exponent $\beta \sim 0.7$ also at $\phi = \phi_c$. The exponent β apparently decreases as τ_b increases: for very small τ_b one recovers a long time exponential decay whereas the decay is less and less exponential for longer bond lifetimes. This suggests that the

stretched exponential decay should be due to the presence of long living structures. β does not seem to vary significantly as the concentration varies around ϕ_c , and this has been observed for all the values of τ_b studied.

For high monomer concentrations we fit the curves for $f_{\bar{q}}(t)$ using the mode-coupling β -correlator [12], corresponding to a short time power law $\sim f + \left(\frac{t}{\tau_s}\right)^{-a}$ and a long time von Schweidler law $\sim f - \left(\frac{t}{\tau_l}\right)^b$. In Fig.6 we show the agreement between the fit (the full lines) and the data for $\tau_b = 1000$ in the range of concentration $\phi = 0.8 - 0.9$. The exponents obtained are $a \sim 0.33 \pm 0.01$ and $b \sim 0.65 \pm 0.01$. At long times the different curves obtained for different ϕ collapse onto a unique master curve by opportunely rescaling the time via a factor $\tau(\phi)$ (Fig.7). The master curve is well fitted by a stretched exponential decay with $\beta \sim 0.50 \pm 0.06$. The characteristic time $\tau(\phi)$ diverges at a value $\phi_g \sim 0.963 \pm 0.005$ with the exponent $\gamma \sim 2.33 \pm 0.06$ (Fig.8). This value well agrees with the mode-coupling prediction $\gamma = 1/2a + 1/2b$ [12].

The same behavior and the same level of agreement between the data and the mode coupling predictions have been obtained for different values of τ_b ($\tau_b = 100, 200, 400, 1000, 3000$). Neither the exponents a and b obtained by the β -correlator nor the exponent β of the stretched exponential vary significantly as function of ϕ and of τ_b . The value of ϕ_g , where the characteristic time $\tau(\phi)$ apparently diverges, seems instead to vary with τ_b , but in any case it is not too far from $\phi_g = 1$.

This glassy relaxation pattern suggests that also in this case the relaxation takes place by means of a caging mechanism: particles are trapped in a cage formed by the surrounding ones, the first relaxation step is due to movements within this cage, whereas the final relaxation is possible due to cage opening and rearrangement. We notice that, as opposed to the usual behavior observed in super-cooled liquids and predicted by the Mode-Coupling Theory, the value of the plateau of the relaxation functions, which is typically related to the size of the cage, strongly depends on the monomer concentration ϕ . This effect will be explained later in terms of effective clusters.

IV. THE RELAXATION TIME AND THE ROLE OF EFFECTIVE CLUSTERS

We study now the relaxation times that can be obtained from the $f_{\bar{q}}(t)$, as the time τ such that $f_{\bar{q}}(\tau) \sim 0.1$. In Fig.9 the relaxation time τ is plotted as function of the monomer concentration ϕ for the permanent bonds and for the finite lifetime bonds case at different values of τ_b . In the figure one finds the data for the permanent bond case on the left, and then from left to right the data for finite bond lifetime, for decreasing values of τ_b .

In the case of permanent bonds (chemical gelation), $\tau(\phi)$ displays a power law divergence at the percolation threshold ϕ_c . For finite bond lifetime τ_b the re-

laxation time instead increases following the permanent bond case, up to some value ϕ^* and then deviates from it. The longer the bond lifetime the higher ϕ^* is. For higher ϕ the increase of the relaxation time corresponds to the onset of the glassy regime in the relaxation behavior, discussed in the previous section. This truncated critical behavior followed by a glassy-like transition has been actually detected in some colloidal systems in the viscosity behavior [35, 36].

We consider now that both in the case of permanent bonds and finite lifetime bonds, clusters of different sizes will be present in the system. In the permanent bond case, a cluster of radius R diffuses in the medium formed by the other percolation clusters, with a characteristic relaxation time $\tau(R)$. At the percolation threshold the connectedness length critically grows in the system and so does the overall relaxation time. In the case of a finite bond lifetime τ_b , it will exist a cluster size R^* so that $\tau_b < \tau(R^*)$. That is, clusters of size $R \geq R^*$ will break and lose their identity on a time scale shorter than $\tau(R)$ and their full size will not contribute to the enhancement of the relaxation time in the system. We can say that the finite bond lifetime actually introduces an effective cluster size distribution with a cut-off and keeps the macroscopic viscosity finite in the system [37].

At high concentrations the system approaches a glassy regime and the relaxation time increases. In order to further investigate the high concentration regime, in Fig.10 we directly compare $f_{\bar{q}}(t)$ at fixed $\phi = 0.85$ for $\tau_b = 10, 100, 400, 1000$, compared to the permanent bond case. We observe that at a fixed value of the monomer concentration ϕ the relaxation functions calculated in the two cases coincides up to times of the order of τ_b . This suggests that on time scales smaller than τ_b the relaxation process must be on the whole the same as in the case of permanent bonds, where permanent clusters are present in the system. That is, for non permanent bonds, this first relaxation is due to relaxation processes that take place over length of the order of the effective cluster radius scales. Over the considered time scale, the system is kinetically arrested in the permanent bond case, once that the percolating cluster is formed. The system with finite τ_b may still relax instead, as the size of the effective clusters is small compared to the sample size. This gives an interpretation in terms of the effective clusters for the two step glassy behavior of the relaxation functions. The first relaxation should be due to the motion of a cluster within the cage formed by the other clusters whereas the second relaxation is due to the cage opening. Therefore the effective clusters play the role of single molecules in an ordinary super-cooled liquid or in a colloidal hard sphere system. This picture supports the jamming of clusters that has been suggested on the basis of experimental observations on colloidal gelation in ref. [16]. The second time scale appears to be of the order of the bond breaking time scale (i.e. τ_b) (Fig.10). This suggests that the cage opening might correspond in this model to the fact that the clusters eventually break. Therefore a

real ergodicity-non-ergodicity transition should only occur only for infinitely large τ_b .

Using this picture of effective clusters, we are able to explain the increase of the plateau in $f_q(t)$. In fact, as different values of the monomer concentration correspond to a different effective cluster size distribution, for each value of ϕ one has a different glassy liquid of effective clusters. This will change the first relaxation and should correspond to the change of the plateau in the relaxation function (Fig.4 and 6). In particular we find that for higher ϕ one has a higher plateau, that is the first decay (the motion of the clusters within the cages) produces a minor relaxation in the system.

V. DIFFUSION PROPERTIES

We obtain further information on the dynamics by the diffusion properties of particles. We calculated the mean square displacement of all the particles $\langle \vec{r}^2(t) \rangle = \frac{1}{N} \sum_{i=1}^N \langle (\vec{r}_i(t+t') - \vec{r}_i(t'))^2 \rangle$, since in the model with finite lifetime bonds, clusters continuously evolve in time, and the diffusion coefficient of a single cluster cannot be defined.

In the model with permanent bonds the mean square displacement of the particles $\langle \vec{r}^2(t) \rangle$ presents a long-time diffusive behavior, and the diffusion coefficient decreases but remains finite also above ϕ_c .

In previous papers [18] the diffusion coefficient of clusters with a fixed size was studied. We found that the clusters, whose size is comparable with the connectedness length, present a diffusion coefficient going to zero at ϕ_c (with the same exponent as the relaxation time), whereas single monomers present a finite diffusion coefficient also in the gel phase. This is due the fact that small clusters are able to escape through the percolating cluster as it has a structure with holes over many different length scales close to the percolation threshold. It is therefore clear that the behavior here observed of the mean square displacement is mainly due to the diffusion of single monomers and small clusters. In Fig.11 $\langle \vec{r}^2(t) \rangle$ is plotted as function of the time in a double logarithmic plot for ϕ approaching ϕ_c , in the case of permanent bonds: particles can still diffuse, the diffusion coefficient apparently diminishes with the concentration of monomers. At high concentrations the sub-diffusive regime stays longer and the long time diffusive behavior is hardly recovered.

In Fig.12 we have plotted the data obtained with $\tau_b = 1000$ and $\phi = 0.8, 0.82, 0.85, 0.9$. According to the results just discussed, for low concentrations $\langle \vec{r}^2(t) \rangle$ shows a simple diffusive behavior. The diffusion does not change significantly close to ϕ_c and for high concentrations the behavior observed is similar to the one of glass forming systems, characterized by a plateau. This onset of a glassy regime has been obtained for different values of τ_b and again it indicates a caging mechanism in the dynamics. The asymptotic diffusion coefficient goes to

zero as ϕ approaches ϕ_g (inset of Fig.12), as a power law as function of $(\phi - \phi_g)$, with an exponent close to γ (section IV) in agreement with the Mode Coupling Theory predictions.

As already done with the relaxation functions we directly compare the mean square displacement obtained in the case of permanent bonds and finite bond lifetime. In Fig.13 it is shown for a fixed value of the concentration $\phi = 0.85$ that the two quantities coincides up to time scales of the order of τ_b . For longer times in the system with non permanent bonds the final diffusive regime is recovered. These results are coherent with the behavior of the relaxation functions discussed in the previous section. The first regime is apparently related to the diffusion of effective clusters. Here again the value of the plateau in the diffusion pattern, which gives the size of the cage, varies with the concentration ϕ . For a higher value of the monomer concentration, the size of the cage apparently decreases. This corresponds to larger effective clusters, which have less free space as compared to their size. By means of the qualitative argument used in section IV, one expects that for a longer τ_b the condition $\tau_b < \tau(R^*)$ will be fulfilled by a larger size R^* and on average larger clusters will persist. For the same value of the concentration, the size of the cage should be the same, whereas the *particles* of this glassy system (i.e. the effective clusters) are longer trapped in the cage as the bond lifetime increases (Fig.13).

VI. DISCUSSION AND CONCLUSION

We have studied a model for gelling systems, both in the case of permanent bonds and with finite bond lifetime. The study of the dynamics shows that when bonds are permanent (chemical gelation) the divergence of the relaxation time is due to the formation of a macroscopic critical cluster and the decay of the relaxation functions is related to the relaxation of such cluster. In the case of finite τ_b there is an effective cluster size distribution, with a cutoff in the size. Note that the clusters cannot be easily defined as in the case of chemical gelation. The effective clusters do not coincide with pairwise bonded particles. A cluster can be identified in a statistical sense as group of monomers which keeps its identity (i.e. the bonds unbroken) when diffusing a distance equal to its diameter. The formation of effective clusters leads to an apparent divergence of the relaxation time which is characterized by exponents corresponding to the case of random permanent bonds (random percolation). As the monomer density increases the jamming of effective clusters gives rise to a colloidal glass transition.

In the case $\tau_b \rightarrow \infty$, starting with a random configuration of unbonded monomers one obtains an out of equilibrium state of the type of cluster-cluster aggregation models, which can be representative of colloidal gelation. Ideally this out of equilibrium system is connected to the two lines described above, the pseudo percolation line

and the glassy line. The pseudo percolation line can be detected if the effective cluster size is large enough and it is quite distinct from the glassy line. However both lines interfere at low density and low temperature with the phase coexistence curve.

We would like to thank K. Dawson, G. Foffi, W. Kob, F. Mallamace, N. Sator, F. Sciortino, P. Tartaglia and

E. Zaccarelli for many interesting discussions. This work has been partially supported by a Marie Curie Fellowship of the European Community programme FP5 under contract number HPMF-CT2002-01945, by MURST-PRIN 2002, MIUR-FIRB 2002, and by the INFM Parallel Computing Initiative.

[1] P.J. Flory *The Physics of Polymer Chemistry* Cornell University Press (Ithaca) 1954

[2] P.G. de Gennes *Scaling concepts in polymer physics* Cornell University Press (Ithaca) 1980

[3] M. Adam, D. Lairez, M. Karpasas and M. Gottlieb, *Macromolecules* **30** 5920 (1997)

[4] D. Stauffer *Physica A* **106** 177 (1981)

[5] D. Stauffer, A. Coniglio and M. Adam, *Adv.in Polymer Sci.* **44** 103 (1982)

[6] J.E. Martin, J.P. Wilcoxon and J. Odinek, *Phys. Rev. A* **43** 858 (1991); F. Ikkai and M. Shibayama, *Phys. Rev. Lett.* **82** 4946 (1999); S.Z. Ren and C.M. Sorensen, *Phys. Rev. Lett.* **70** 1727 (1993); P. Lang. and W. Burchard *Macromolecules* **24** 815 (1991)

[7] A.D. Dinsmore and D.A. Weitz *J. Phys. : Condens. Matter* **14** 7581 (2002)

[8] P. Meakin *Phys. Rev. Lett.* **51** 1119 (1983); M. Kolb, R. Botet and R. Jullien *Phys. Rev. Lett.* **51** 1123 (1983)

[9] V. Trappe, V. Prasad, L. Cipelletti, P.N. Segré and D.A. Weitz, *Nature* **411** 772 (2001); V. Trappe and D.A. Weitz, *Phys. Rev. Lett.* **85** 449 (2000)

[10] H. Gang, A. H. Krall, H. Z. Cummins, and D. A. Weitz, *Phys. Rev. E* **59** 715 (1999)

[11] F. Mallamace, P. Gambaudo, N. Micali, P. Tartaglia, C. Liao and S.H. Chen, *Phys. Rev. Lett.* **84** (2000) 5431; S.H. Chen, W.R. Chen, F. Mallamace, *Science* **300** (2003) 619

[12] W. Götze in *Liquid, Freezing and Glass Transition*, eds. J.P. Hansen, D. Levesque and P. Zinn-Justin, Elsevier (1991)

[13] L. Fabbian, W. Götze, F. Sciortino, P. Tartaglia and F. Thiery, *Phys. Rev. E* **59**, R1347 (1999); **60**, 2430 (1999); J. Bergenholtz, M. Fuchs, and Th. Voigtmann, *J. Phys. : Condens. Matter* **12**, 6575 (2000)

[14] K. Dawson, G. Foffi, M. Fuchs, W. Götze, F. Sciortino, M. Sperl, P. Tartaglia, Th. Voigtmann and E. Zaccarelli, *Phys. Rev. E* **63** 011401 (2001); E. Zaccarelli, G. Foffi, K. A. Dawson, F. Sciortino and P. Tartaglia, *Phys. Rev. E* **63**, 031501 (2001)

[15] A.M. Puertas, M. Fuchs and M.E. Cates cond-mat/0211087; M.E. Cates to appear in *Annales Henri Poincaré*; A.M. Puertas, M. Fuchs and M.E. Cates *Phys. Rev. Lett.* **88** (2002) 098301

[16] P. N. Segré, V. Prasad, A. B. Schofield, and D. A. Weitz *Phys. Rev. Lett.* **86** 6042 (2001)

[17] E. Del Gado, A. Fierro, L. de Arcangelis and A. Coniglio *Europhys. Lett.* (2003), in press

[18] E. Del Gado, L. de Arcangelis and A. Coniglio *Eur. Phys. J. B* **2** 352 (2000)

[19] A. Aharony, D. Stauffer *Introduction to percolation theory* Taylor and Francis, London (1994)

[20] I. Carmesin and K. Kremer *Macromolecules* **21** 2819 (1988)

[21] H. P. Deutch and R. Dickman *J. Chem. Phys.* **93** 8983 (1990); H. P. Deutch and K. Binder *J. Chem. Phys.* **94** 2294 (1991)

[22] E. Del Gado, L. de Arcangelis and A. Coniglio *J. Phys. A* **31** 1901 (1998); *Europhys. Lett.* **46** 288 (1999)

[23] E. Del Gado, L. de Arcangelis and A. Coniglio *Phys. Rev. E* **65** 041803 (2002)

[24] Taking into account both the interaction energy by means of τ_b and the frequency f_b for the bonds corresponds to have a free energy barrier in the bond formation [25]: Consider a pair of particles which can be in $\Omega + 1$ configurations. Ω (unbonded) corresponds to zero energy and 1 (bonded) corresponds to energy $-E$. Breaking of a bond corresponds to go from a state of energy $-E$ to a state of entropy $S = K \ln \Omega$, with a variation in the free energy $\Delta F = E - KT \ln \Omega$. The lifetime of the bonding configuration is proportional to $e^{E/KT}$, and the frequency to go from one of the unbonding configurations to the bonding configuration is given by $f_b = \frac{1}{\Omega}$.

[25] A. Coniglio, H.E. Stanley, W. Klein *Phys. Rev. B* **25** (1982) 6805

[26] We consider one starting configuration with a fixed ϕ as obtained in the case of permanent bonds. For each value of the bond lifetime τ_b we perform test simulations for different values of f_b . The fraction of formed bonds respect to all the possible ones varies during an initial transient and then fluctuates around an average value which, for a fixed ϕ , depends on τ_b and f_b . For the study of the dynamics, for each value of τ_b we take the f_b so that the average value of the fraction of present bonds during the simulations is the same as its value at the same ϕ with permanent bonds.

[27] The role of directional effects in the attractive interaction in colloidal gels is not clear and is worth to be further investigated.

[28] R. Jullien and A. Hasmay *Phys. Rev. Lett.* **74** 4003 (1995)

[29] M. Kolb and R. Jullien, *J. Phys. (Paris) Lett.* **45**, L977 (1984); F. Family, P. Meakin, and T. Vicsek, *J. Chem. Phys.* **83**, 4144 (1985).

[30] The errors are calculated as the fluctuations on the statistical ensemble (obtained varying the random number generator in our simulations). Where not explicitly shown, the error bars are of the order of the symbol size in figures.

[31] E. Del Gado, A. Fierro, L. de Arcangelis and A. Coniglio in preparation.

[32] A. T. Ogielski *Phys. Rev. B* **32** 7384 (1985).

[33] A. Parker and V. Normand cond-mat/0306056.

[34] Although with these two conditions we cannot exclude that we are in an aging regime, we do not expect to find aging, as we are not in the glassy region [31].

- [35] F. Mallamace, S.H. Chen, Y. Liu, L. Lobry and N. Micali, *Physica A* **266** (1999); F. Mallamace, R. Beneduci, P. Gambadauro, D. Lombardo and S.H. Chen, *Physica A* **302** 202 (2001)
- [36] F. Lafleche, D. Durand and T. Nicolai *preprint* (2002)
- [37] A. Coniglio *J. Phys. : Condensed Matter* **13** 9039 (2001)

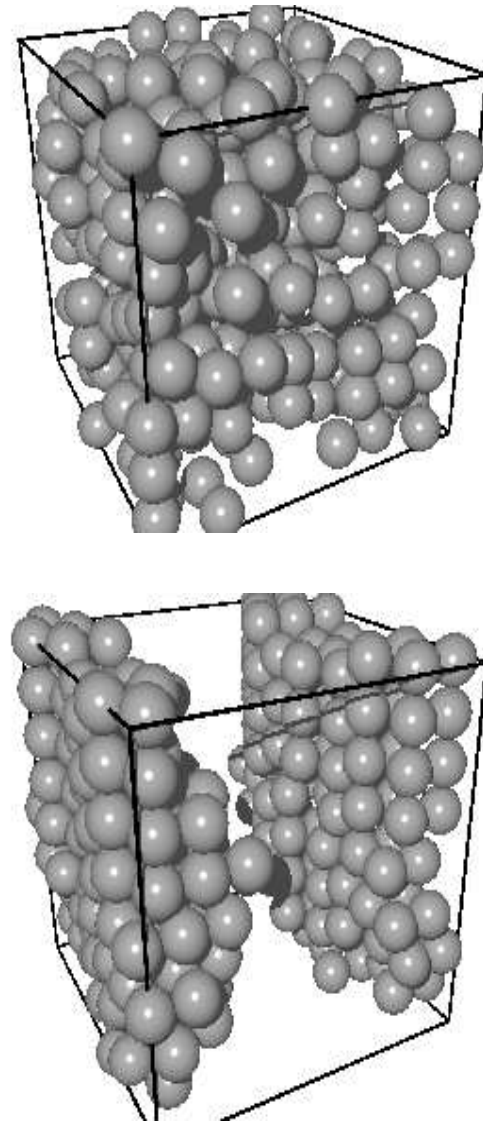


FIG. 1: Two typical configurations obtained for $\phi = 0.6$ with $\tau_b = 100$ and $f_b = 0.02$ (a), where there is no evidence of phase separation, and with $\tau_b = 2$, $f_b = 1$ and monomers of valence 6 (b), where the phase separation occurs.

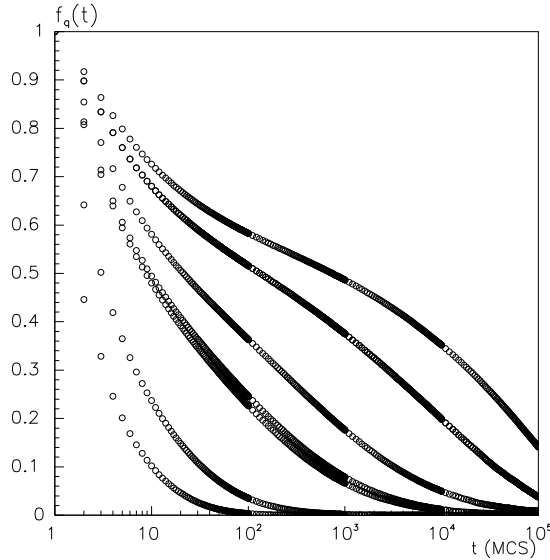


FIG. 2: The relaxation functions for permanent bonds $f_{\bar{q}}(t)$ as function of the time for $q \sim 1.36$ and, from left to right, $\phi = 0.5, 0.6, 0.68, 0.718, 0.75, 0.8, 0.85$.

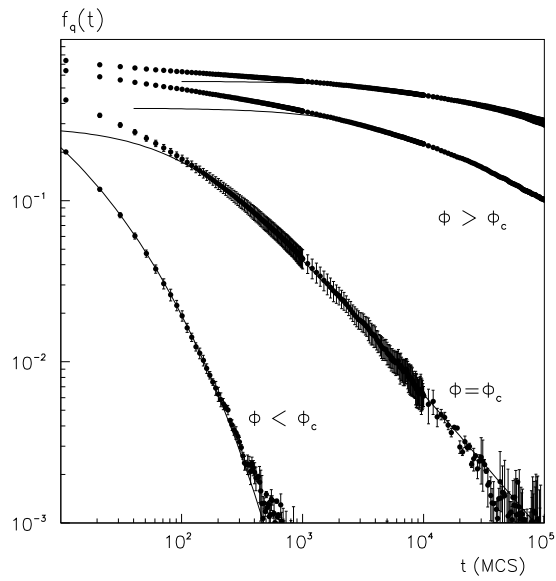
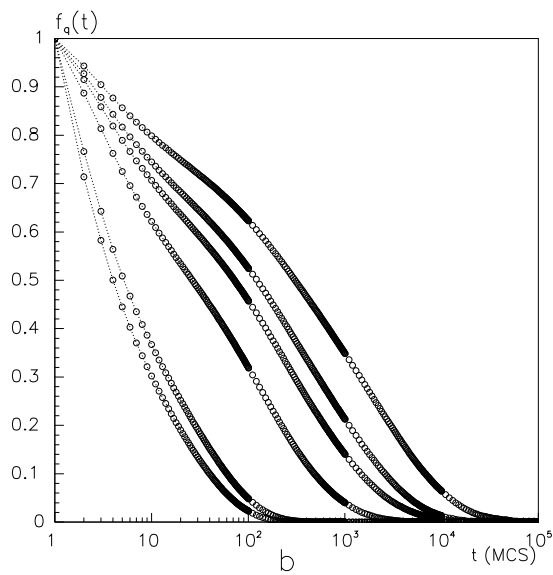
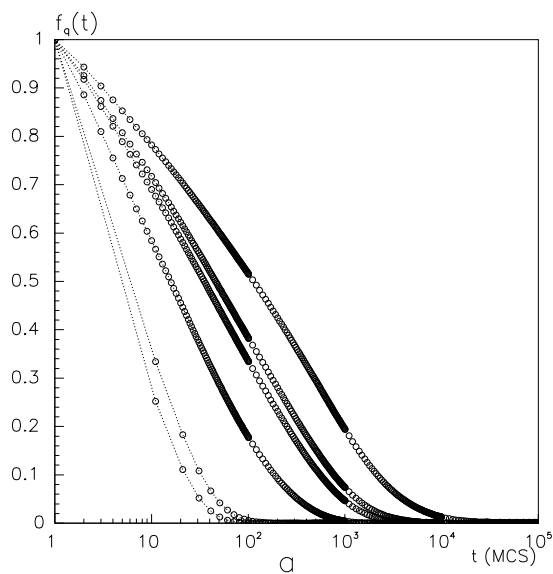


FIG. 3: Double logarithmic plot of the autocorrelation functions $f_{\bar{q}}(t)$ as function of the time for $q \sim 1.36$ and $\phi = 0.6, 0.718, 0.8, 0.87$. For $\phi < \phi_c$ the long time decay is well fitted by a function (full line) $\sim e^{-(t/\tau)^\beta}$ with $\beta \sim 0.3$. At the percolation threshold and in the gel phase in the long time decay the data are well fitted by a function $\sim (1 + \frac{t}{\tau})^{-c}$.



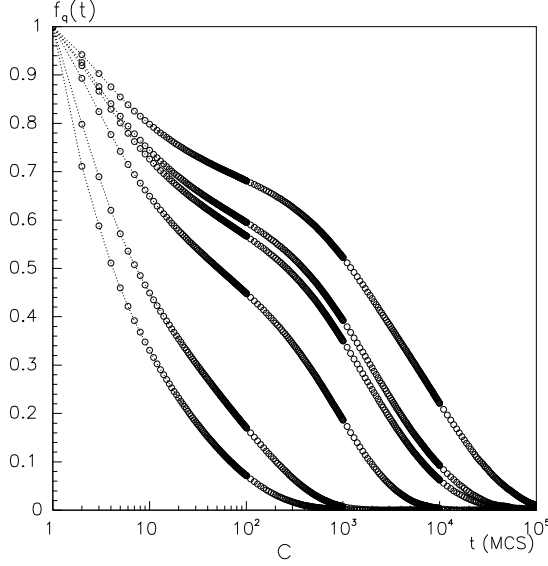


FIG. 4: $f_{\bar{q}}(t)$ as function of the time for $q \sim 1.36$ calculated on a cubic lattice of size $L = 16$: for $\phi = 0.6, 0.7, 0.8, 0.85, 0.87, 0.9$ (from left to right) and $\tau_b = 10MCstep/particle$ (a); $\tau_b = 100MCstep/particle$ (b); $\tau_b = 1000MCstep/particle$ (c); the dotted lines are a guide to the eye.

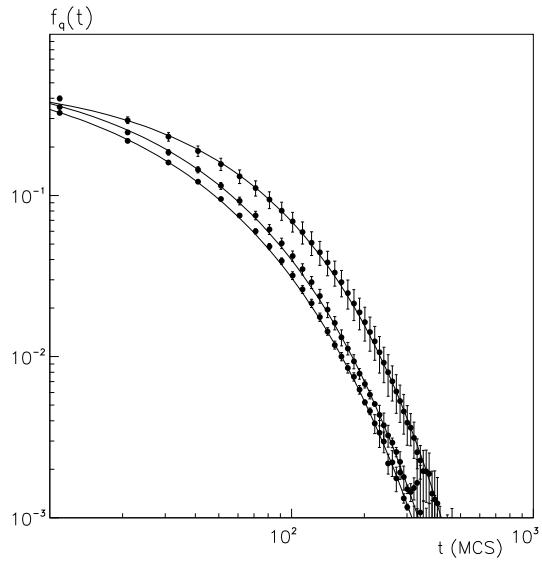


FIG. 5: The long time decay of $f_{\bar{q}}(t)$ in a log-log plot for $q \sim 1.36$. It has been calculated on a cubic lattice of size $L = 16$ for $\tau_b = 100MCstep/particle$ (from left to right $\phi = 0.65, 0.68, 0.718$). The data are fitted using a stretched exponential function with $\beta \sim 0.7$ (full lines).

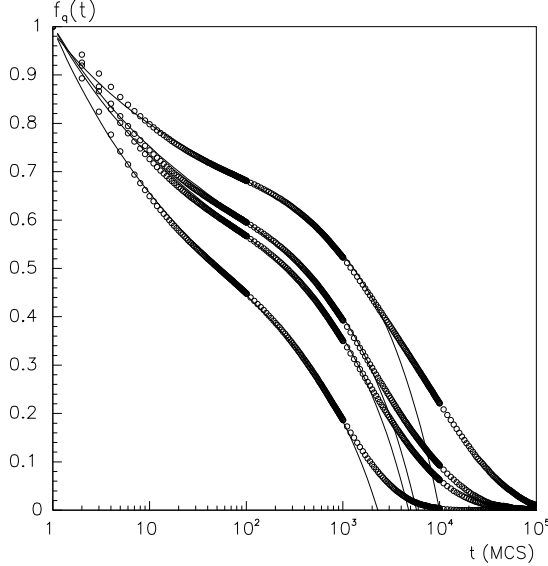


FIG. 6: $f_{\bar{q}}(t)$ as function of the time for $q \sim 1.36$ calculated on a cubic lattice of size $L = 16$ for $\tau_b = 1000MCstep/particle$. From left to right $\phi = 0.8, 0.85, 0.87, 0.9$. The full lines correspond to the fit with the β -correlator.

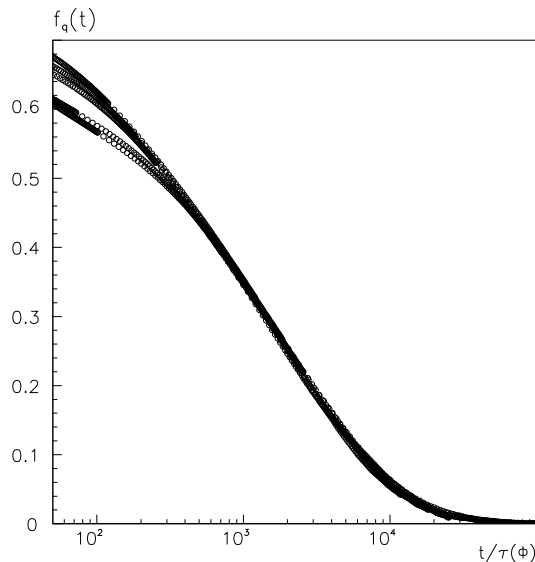


FIG. 7: $f_{\bar{q}}(t)$ obtained for $q \sim 1.36$, $\tau_b = 1000$, and $\phi = 0.85, 0.87, 0.9, 0.91, 0.92$: by opportunely rescaling them by a quantity $\tau(\phi)$ they collapse into a unique master curve, well fitted by a stretched exponential function with $\beta \sim 0.5 \pm 0.06$.

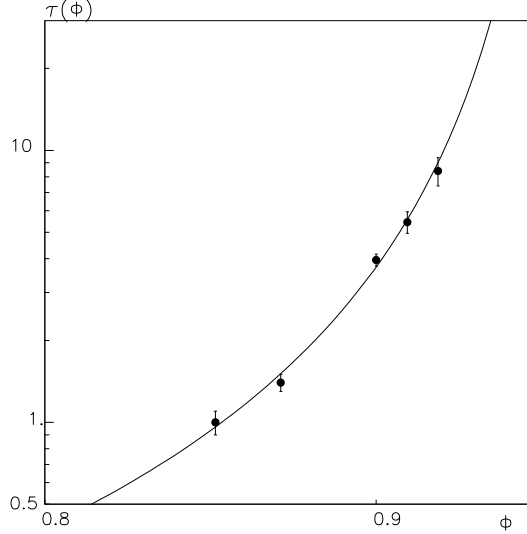


FIG. 8: Log-log plot of the characteristic time $\tau(\phi)$ obtained by the rescaling of the relaxation functions. The points have been fitted (full line) with the function $0.006(\phi - \phi_g)^{-2.33}$, where $\phi_g \sim 0.96 \pm 0.01$.

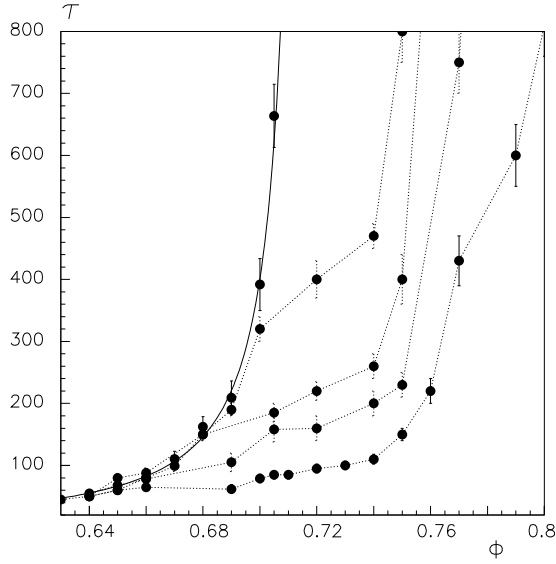


FIG. 9: The average relaxation time as function of the density; from left to right: the data for the permanent bond case diverge at the percolation threshold with a power law (the full line); the other data refer to finite $\tau_b = 3000, 1000, 400, 100 MCstep/particle$ decreasing from left to right (the dotted lines are a guide to the eye).

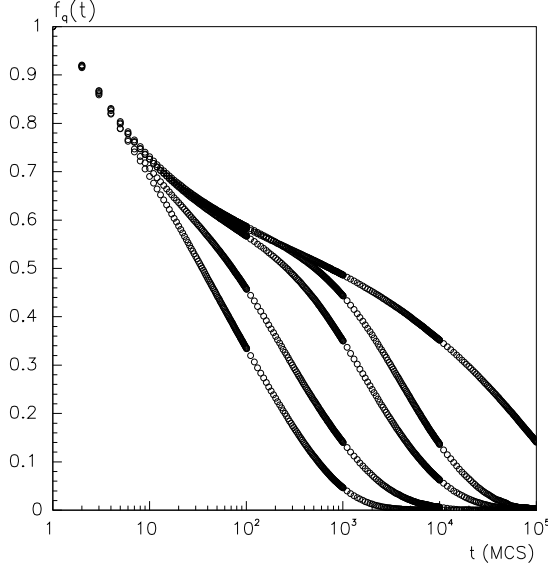


FIG. 10: $f_{\bar{q}}(t)$ obtained for $\phi = 0.85$ and $q \sim 1.36$: the different curves refer to $\tau_b = 10, 100, 400, 1000$, compared to the permanent bond case (from left to right).

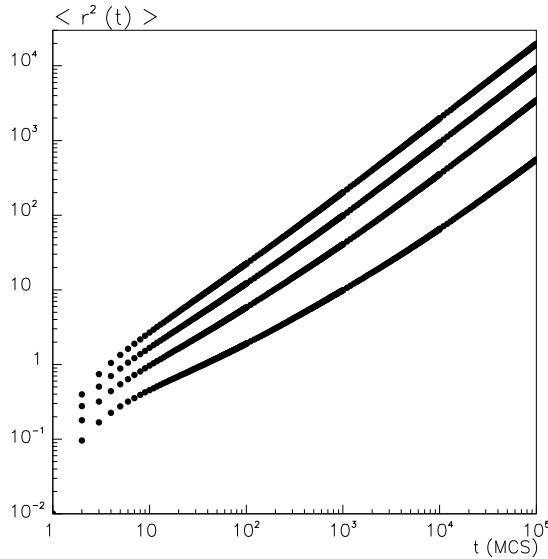


FIG. 11: The mean-square displacement $\langle \bar{r}^2(t) \rangle$ of the particles as function of the time in a double logarithmic plot for permanent bonds: from top to bottom $\phi = 0.4, 0.5, 0.6, 0.7$, approaching ϕ_c .

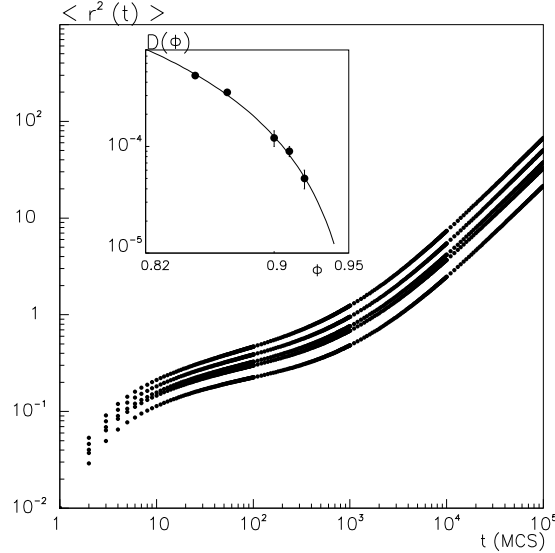


FIG. 12: The mean-square displacement $\langle \vec{r}^2(t) \rangle$ of the particles as function of the time in a double logarithmic plot for $\tau_b = 1000MCstep/particle$: from top to bottom $\phi = 0.8, 0.82, 0.85, 0.87, 0.9$, approaching $\phi_g(\tau_b)$. In the inset, the diffusion coefficient: the full line is the fit with the function $\sim (0.963 - \phi)^{-2.3}$.

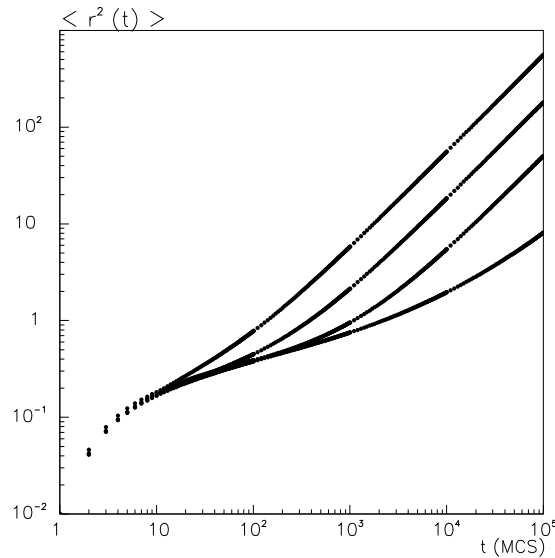


FIG. 13: The mean-square displacement $\langle \vec{r}^2(t) \rangle$ of the particles as function of the time in a double logarithmic plot, obtained at $\phi = 0.85$. The different curves, from top to bottom, refer to $\tau_b = 10, 100, 1000$ and the case of permanent bonds.